

Cell damage in UVA and CW/Femtosecond NIR microscopes

Karsten König¹, Hong Liang², Sol Kimel³, Lars O. Svaasand⁴, Bruce J. Tromberg²,
Tatjana Krasieva², Michael W. Berns², Karl-Jürgen Halbhauer¹,
Peter T.C. So⁵, William W. Mantulin⁵, Enrico Gratton⁵

¹Institute of Anatomy II, Friedrich Schiller University, D-07743 Jena, Germany

²Beckman Laser Institute and Medical Clinic, University of California, Irvine, CA 92715

³Dept. of Chemistry, Technion-Israel Institute of Technology, Haifa 32000, Israel

⁴Norwegian Institute of Technology, University of Trondheim, N-7034 Trondheim, Norway

⁵Laboratory of Fluorescence Dynamics, Dept. of Physics, University of Illinois, Urbana

1. ABSTRACT

Cell damage in UV and NIR laser microscopes by highly focused micromanipulation and fluorescence excitation microbeams has been studied. Damage in erythrocytes, spermatozoa and Chinese hamster ovary cells was detected by monitoring morphology changes, autofluorescence detection, cloning assay, and viability screening. It was found that 364nm/365 nm UVA radiation induced irreversible cell damage at radiant exposures as low as $<10 \text{ J/cm}^2$. NIR CW microradiation used in laser tweezers was also able to damage cells via a two-photon excitation process, in particular, when using $<800\text{nm}$ trapping beams. Non-destructive two-photon excitation in femtosecond NIR microscopes is possible within a narrow intensity window. The lower limit is determined by two-photon absorption coefficients and detector efficiency, the higher by intracellular optical breakdown in the extranuclear region. Above certain wavelength-dependent intensity thresholds in femtosecond microscopy, cells were completely destroyed by fragmentation concomitant with plasma generation. The influence of excitation and micromanipulation microbeams should be considered when studying physiology and metabolism of vital cells.

Keywords: laser tweezers, cell damage, two-photon microscopy, femtosecond, NIR

2. INTRODUCTION

The combination of ultraviolet (UV) and visible (VIS) laser radiation with optical microscopy led to new diagnostic methods in cellular and molecular biology such as 3D-imaging by confocal laser scanning microscopy (CLSM), high-resolution imaging by scanning near field optical microscopy (SNOM) and fluorescence lifetime imaging with sub-nanosecond temporal resolution. Intracellular sterile microsurgery became possible with the application of powerful pulsed laser beams in microscopy.

A novel direction in modern cell microscopy is near infrared (NIR) laser microscopy using 700 nm - 1100 nm laser wavelengths. Important applications of NIR-microscopy are cellular force measurements and cellular/molecular micromanipulations by continuous wave (CW) optical traps (laser tweezers)^{1,2}. NIR traps are based on the radiation pressure of highly-focused laser beams. The second important application of NIR microscopy is femtosecond two-photon microscopy for fluorescence imaging and the release of "caged" compounds based on nonresonant, nonlinear excitation of cellular chromophores with UV and VIS electronic transitions by the simultaneous absorption of two NIR photons³.

In most laser microscopes, the laser beam is focused to its diffraction-limited spot size $d \approx \lambda/\text{NA}$ (λ : laser wavelength, NA: numerical aperture of the objective). Using high numerical aperture objectives ($\text{NA}>1$), spots are in the sub-micron region. The highly-focused laser beams are termed microbeams.

We studied the influence of CW UVA and NIR microbeams as well as of femtosecond NIR microbeams on cell metabolism and viability.

3. MATERIALS AND METHODS

Cells

Chinese hamster ovary cells (CHO, ATCC no. 61) were maintained in GIBCO's minimum essential medium (MEM, 10% fetal bovine serum). Cells were grown in modified sterile Rose cell culture chambers. Light-exposed interphase cells were monitored for their clonal growth up to 5 days after phototreatment. CHO cells were considered unaffected by light if clones consisting >50 cells were produced. Semen specimens were obtained from donors with normal semen parameters according to the World Health Organization guidelines. Semen was diluted in HEPES buffered isotonic saline solution containing 1% human serum albumin and injected into similar microchambers. Peripheral human blood was freshly drawn from a finger of a healthy donor and diluted in a PBS-glucose-heparin solution. In vitality experiments, cells were stained with a Live/Dead kit (Molecular Probes) containing the live-cell stain SYBRTM14 with a 515 nm fluorescence maximum and the dead-cell stain Propidium Iodide (PI) emitting in the red.

Microbeams

UVA microbeams were provided by an Ar⁺-laser (Stabilite 2017-06S, ≈35 mW output power at 363.8 nm, Spectra Physics) combined with a Zeiss CLSM (Axiovert 135M). For comparison, the 365nm radiation of a standard 50 W high-pressure mercury lamp of fluorescence microscopes was used.

The CW NIR radiation of an Ar⁺-ion laser-pumped tunable CW Ti:Sapphire ring laser (Coherent, 899-01) was introduced into a modified inverted confocal laser scanning microscope (CLSM, Axiovert 135M, Zeiss). The parallel beam was expanded to fill the back aperture of a 100x Zeiss Neofluar brightfield objective (NA=1.3). In addition, a CW Nd:YAG laser was used as trapping source. The microscope allowed trapping of single cells and simultaneous fluorescence imaging; either by scanning with 488 nm argon ion laser microbeams, by detection with a slow-scan, cooled CCD camera (TE576/SET135, Princeton Instruments), or by sensitive color video imaging (ZVS-47DEC, Zeiss).

Femtosecond NIR radiation was provided by a tunable mode-locked Ti:sapphire laser (Mira 900, Coherent) operating at a pulse width of ≈150 fs and a 80 MHz repetition frequency. The beam was launched into a Zeiss confocal laser scanning microscope or into a fluorescence microscope with external 1 kHz x,y-scanner and focused to a diffraction-limited spot by a 63x Neofluar objective (NA=1.25).

Transmittance T and pulse broadening M due to group velocity dispersion of the Zeiss objectives were determined by a sandwich-setup consisting of two identical objectives and a Rose microchamber (filled with medium) as well as a power meter and an autocorrelator (Fig. 1). Typical values of the system: 100x objective (NA=1.3) and Rose chamber for 800nm beams were T = 0.6 and M = 5% (≈2000 fs²).

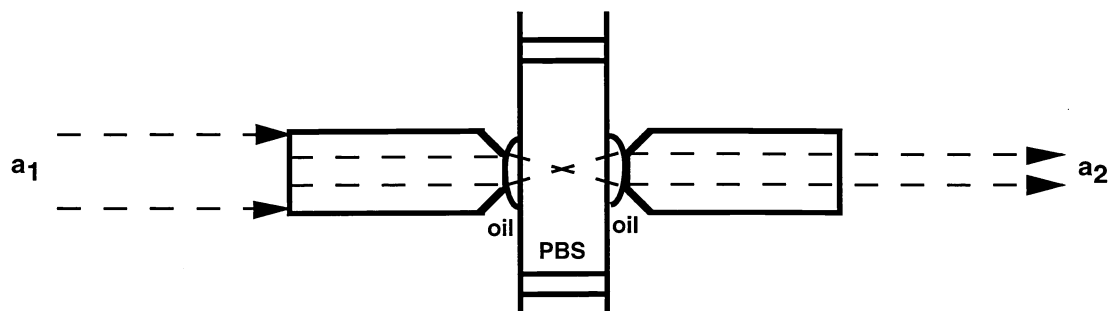


Fig. 1 Sandwich setup for transmittance T and optical dispersion OD determination of high-NA objectives. The objectives were aligned in a distance twice the focal length. The power of the transmitted parallel beam reflects T² and 2·OD (chirp-free pulse).

4. RESULTS

4.1. Cell damage in UVA microscopes

Highly focused CW UVA Ar⁺ laser beams (63x, NA=1.25) at 364 nm of a UV Zeiss CLSM have been used to study damage effects in CHO cells. For that purpose, adherent single CHO cells were scanned 10 times in a 256x256 pixel field at 80 μ s pixel dwell time. Cells were marked with a diamond on the lower cell chamber window to ensure 5 days monitoring of clonal growth. Starting with mW powers, no UV exposed cell survived. Laser powers >20 μ W inhibited normal cell division. At a power of 6 μ W, 50% of the cells exhibited normal clonal growth (2 divisions per day). The other exposed cells died or produced giant cells. With a spot size of $\lambda/NA \approx 290$ nm, the intensity and the fluence of the 6 μ W-microbeam was ≈ 9 kW/cm² and 7.2 J/cm² (10 scans), respectively.

For comparison, single CHO cells were exposed to 365nm lamp light. A power of ≈ 1 mW (100x, NA=1.3) and a "spot" size of 190 μ m resulted in 3.5 W/cm² intensity. As indicated in Fig. 2, 10 s UVA exposure (35 J/cm²) inhibited normal cell growth in all cells. 50% cloning efficiency was determined for ≈ 1 s exposure time. The lamp results confirm the damaging effect for fluences as low as <10 J/cm² obtained in laser microbeam studies. Additional tests (autofluorescence studies, viability test, comet assay) on CHO cells demonstrated disturbances in the intracellular redox state due to NADH-attributed autofluorescence modifications, DNA strand breaks and loss of viability for J/cm² UVA fluences⁴. Spermatozoa exposed to 365nm lamp radiation exhibited paralysis, onset of NADH-attributed autofluorescence in the sperm head, and finally cell death within 5 min of exposure.

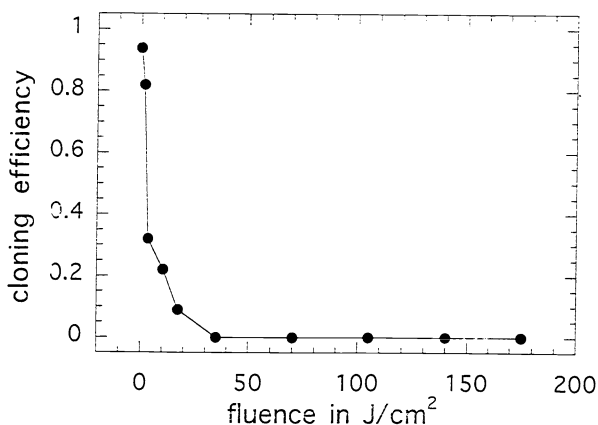


Fig. 2 Cloning efficiency of 365nm-exposed CHO cells vs. laser fluence.

4.2. CW NIR microbeam induced cell damage

Trapping of human spermatozoa with 105 mW laser tweezers of the multimode CW Ti:sapphire laser at <800nm wavelengths resulted in trap-induced paralysis, disturbances in the intracellular redox state (autofluorescence modifications), and in cell death. The most destructive effect occurred at 760 nm (cell death after 65 ± 20 s). In contrast, longer-wavelength traps (800nm, 1064 nm) showed no damaging effect during a 10 min trapping period (Fig. 3). Powers of ≈ 100 mW (minimum trapping power) are necessary to confine highly motile cells in the trap.

The intensity in the trapping spot ($d \approx \lambda/NA$) was ≈ 40 MW/cm². Therefore, cell damage by 760nm traps occurred at ≈ 2 GJ/cm² fluence. Fluences of > 20 GJ/cm² did not harm cells confined in 1064nm-traps.

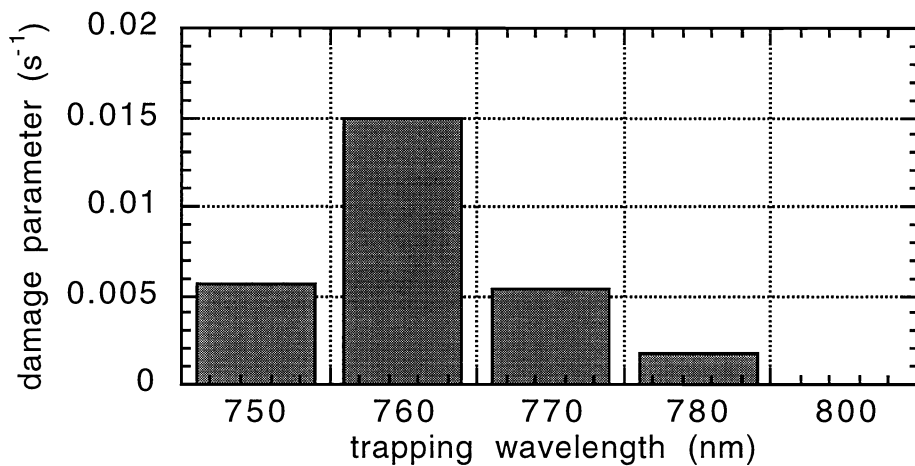


Fig. 3 Action spectrum of trap-induced spermatozoa damage. The reciprocal value of the trapping time where onset of PI accumulation occurred was used as damage parameter.

Human erythrocytes confined in NIR traps suffered from "heat-induced" membrane damage and hemolysis. Damage showed a dependence on wavelength and on trapping time. At 800 nm, fluences of $\approx 1 \text{ GJ/cm}^2$ were required to induce cell damage. Non-destructive erythrocyte trapping over a 2 min trapping period was possible for powers $< 50 \text{ mW}$ at wavelengths $> 740 \text{ nm}$ (Fig. 4). Powers of $< 5 \text{ mW}$ were sufficient to confine erythrocytes in the trap. Therefore, non-destructive optical erythrocyte micromanipulation is feasible within a wide power/energy range. Non-trapped cells in a heating bath were found to be hemolysed within 2 min between 50°C (4% of cells hemolysed) and 62°C (100% hemolysed).

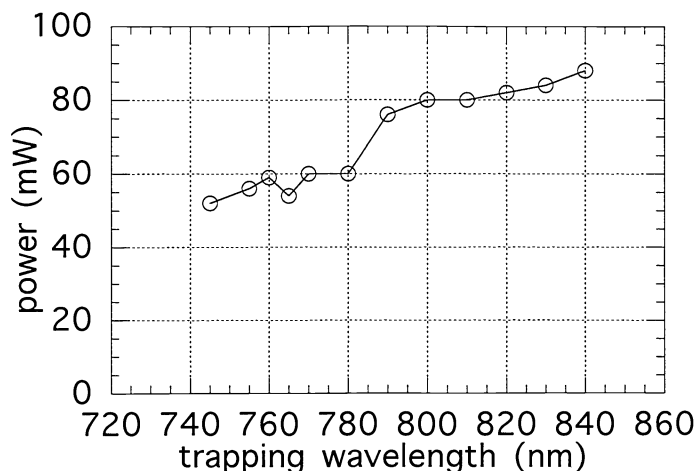


Fig. 4 Trap-induced hemolysis of human erythrocytes. Minimum trapping power required to lyse cells within 2 min (room temperature: 26°C) vs. trapping wavelength.

CHO cells in a 760nm-trap (160 mW) exhibited, in the first minutes of trapping, significant NADH-attributed autofluorescence modifications indicating changes in cellular redox state. In contrast, one hour 1064nm trapping (230 mW, 100 GJ/cm²) revealed no autofluorescence changes⁵. Exposure of adherent CHO cells (no trapping) with 90 mW microbeams (multimode CW Ti:sapphire laser) showed reduced cloning efficiency, giant cell formation, and cell death. The strongest damaging effect was found at 760 nm. A 50% cloning efficiency was determined after ≈5 s exposure (≈0.16 GJ/cm²) at this wavelength. No cell was able to divide after 1 min exposure (Fig. 5). Transformation of the multimode CW laser into a single-frequency laser by introduction of an intracavity 20 MHz etalon reduced the damaging effect. For example, human spermatozoa could now be confined as long as 400±100 s in 760nm traps without PI accumulation indicating cell death. The effect of single-frequency traps on cloning efficiency of CHO cells is seen in Fig. 5.

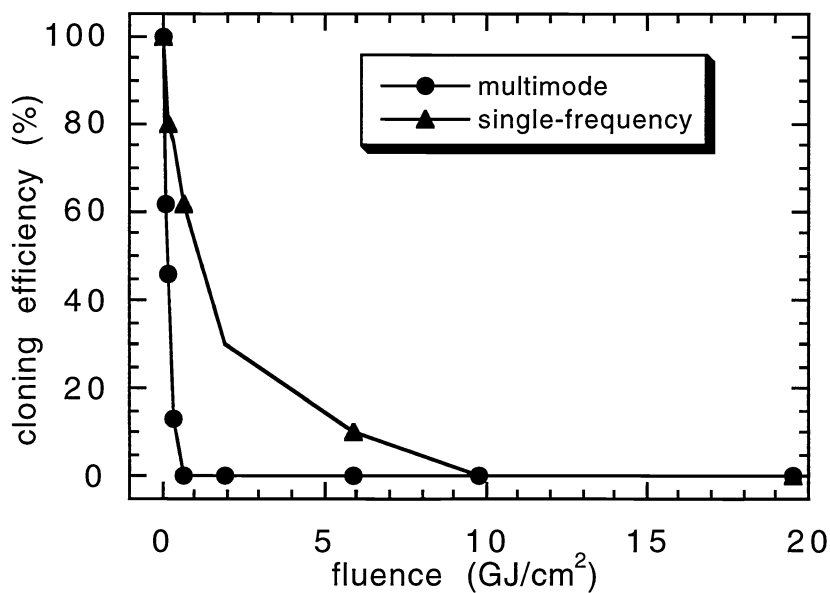


Fig. 5 CHO cloning efficiency vs. fluence at 760nm (90 mW).

4.3. Femtosecond NIR microbeam induced cell damage

We were not able to confine vital spermatozoa with femtosecond microbeams at 100 mW average power. Hit by the beam, sperm heads "exploded" and the flagellum ruptured. We decreased the mean power down to 6 mW. At that power, motile sperm cells could not be confined. We scanned (730 nm, 256x256 pixel field at 80 μs pixel dwell time) a single non-motile sperm cell of a donor with infertility. The first scan revealed NADH-attributed two-photon excited autofluorescence in the cell midpiece where mitochondria are located. However, the second scan showed fluorescence relocation. The sperm head became the brightest fluorescent side. Such photoinduced autofluorescence modifications have been found also during CW UVA and NIR exposure.

Human erythrocytes showed no changes in morphology and viability for mean powers <2 mW during scanning with femtosecond microbeams. However, higher powers resulted in discocytic-echinocytic shape transformation. Powers ≥5 mW led to transformation into spheres and hemolysis in dependence on the number of scans and pixel dwell time.

Scanning of CHO cells (256x256 pixel field at 80 μs pixel dwell time) revealed no changes in morphology nor in cloning efficiency if the average power remained below 2 mW. However, higher

powers led to giant cell formation, reduced cloning efficiency, and cell death. At a power of >6 mW (730-800 nm) cells showed bright short-lived (<500 ps) white luminescence in the mitochondrial region⁶. The luminescence formation was accompanied by cell fragmentation. There was no dependence on number of scans, indicating a power dependence and not a fluence dependence (Fig. 6).

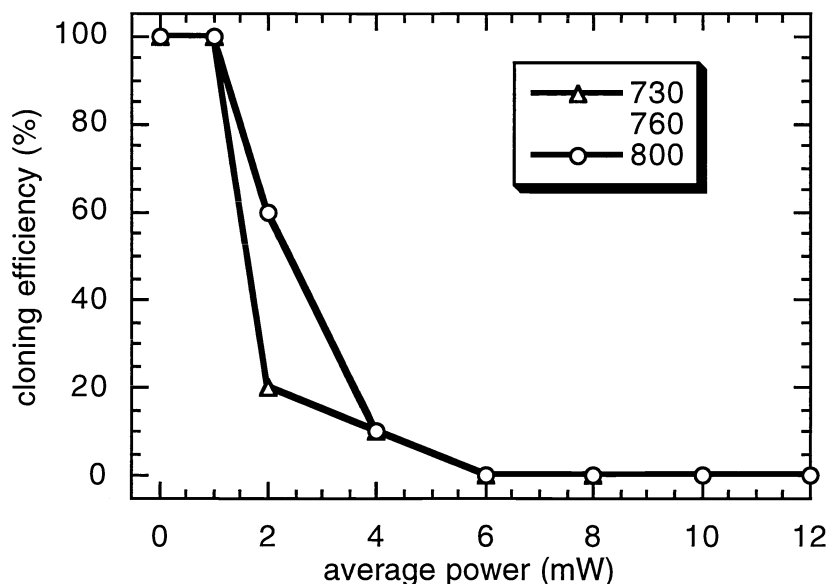


Fig. 6 CHO cloning efficiency vs. mean laser power after femtosecond NIR exposure

5. DISCUSSION

Laser microbeams have been widely employed in biology, biotechnology, and medicine as non-contact sterile tools for cell and biomolecule diagnostics and micromanipulation. As demonstrated, UVA and NIR microbeams have the potential to harm vital cells.

UVA microbeams at 364/365 nm, used as excitation radiation in fluorescence microscopes, were found to damage cells at fluences as low as 10 J/cm^2. Such fluences are obtained during exposure times of seconds when high-NA-objectives are used. UVA (320-400 nm) is well known to induce genetic as well as nongenetic damage via oxidative stress due to the formation of reactive oxygen species (i.e., singlet oxygen and oxygen radicals)^{7,8}.

Intensities in the MW/cm^2 region occur during NIR trapping of vital cells. Cells with no chlorophyll, melanin, or hemoglobin do not absorb NIR efficiently. For example, the water absorption coefficient at 1064 nm is only $\approx 0.1 \text{ cm}^{-1}$. Indirect, intracellular temperature measurements using a thermosensitive fluorophore revealed a minor trap-induced temperature increase of <math><2 \text{ K}</math> in the case of CHO cells and spermatozoa (1064 nm, 100 mW)⁹. Significant heating is expected in the case of trapped erythrocytes (cell dimension $2R \approx 8 \mu\text{m}$) with an estimated hemoglobin absorption coefficient of $\alpha \approx 30 \text{ cm}^{-1}$ (730 nm). Indeed, trap-induced hemolysis within 2 min was found at >50 mW power. However, such high powers are not required for erythrocyte trapping. The trap-induced temperature increase can be estimated as follows:

The generation of thermal energy per unit time Q_{heat} by optical absorption can be expressed,

$$Q_{\text{heat}} = P(1 - e^{-2.3\alpha 2R}) \approx 2.3P\alpha 2R \approx 0.06P$$

The temperature rise T for an erythrocyte can be approximated with the temperature rise for uniformly distributed power within a sphere. The temperature rise at the perimeter can then be expressed,

$$q = Q_{\text{heat}}/(4\pi R^2) = -\kappa dT/dr \quad T(r) = Q_{\text{heat}}/(4\pi\kappa r)$$

$$T(r=R) = Q_{\text{heat}}/(4\pi\kappa R) \approx P \cdot 2.3\alpha/(2\pi\kappa) \quad \text{with } \kappa \approx 0.6 \text{ W/mK (water)}$$

A 5 mW trapping power is sufficient to confine single erythrocytes in the focal volume of a high-NA-objective. At that power, the calculation gives ≈ 9 K temperature increase at the perimeter.

The photomechanical stress generated by optical force formation in laser tweezers of $P = 100$ mW is not responsible for the detected trap-induced damage of CHO cells and spermatozoa at < 800 nm trapping wavelengths. With trapping parameters $Q < 0.2$, the optical force $F = QP/c$ (c : light velocity in medium) is on the order of pN and, therefore, in the region of cellular forces (e.g. motility force of spermatozoa). Therefore, traps can be used for cell force measurements^{10,11}.

The observed cell damage in short-wavelength NIR traps is based on non-resonant two-photon excitation of endogenous chromophores, such as NADH. When 50-150 mW CW laser beams are focused to diffraction-limited spots, trapping intensities of 15-40 MW/cm² (750-1064 nm) corresponding to photon flux densities of $\approx 10^{27}$ cm⁻²s⁻¹ are generated. With typical 10⁻⁵⁰ cm⁴s molecular two-photon absorption cross sections^{10,11}, two-photon excitation processes are efficiently induced¹². Due to the squared dependence of two-photon excitation on laser power, two-photon effects are amplified in multimode CW-lasers where transient power fluctuations occur as a result of longitudinal mode beating. Interestingly, highest transient power levels in the multimode CW Ti:sapphire ring laser were obtained at 760 nm (partial mode locking)¹³. Therefore, "amplified" cell damage occurred in 760 nm multimode traps. Action spectra (700 nm - 1064 nm) of CHO damage due to multimode CW microirradiation were published recently¹⁴.

The intensity and photon flux density of femtosecond microbeams within the time of pulse interaction with cellular structures are on the order of 100 GW/cm² - TW/cm² and $\approx 10^{31}$ - 10^{32} photons cm⁻²s⁻¹, respectively, for typical laser parameters (150 fs, 100 MHz, 1-10 mW average power) in two-photon microscopes¹⁵. Therefore, extremely high electric fields on the order of MV/cm are generated which could induce first optical breakdowns in the target. For example, typical threshold values for the femtosecond pulses induced onset of plasma formation are 10¹³ W/cm² (60 MV/cm) in glass¹⁶ and 10¹¹ W/cm² in water¹⁷. Optical breakdown in glasses was found to be induced in locations of small contaminations or scratches¹⁶. As shown by our experiments, plasma occurred in the mitochondrial region. Onset of plasma did not start in the extracellular medium or the nucleus. Mitochondria contain efficient two-photon absorbers, e.g. porphyrins and fluorescent coenzymes. The destruction effect was shown to be electric field dependent. Therefore, non-destructive two-photon microscopy of living cells is limited to a narrow intensity window. The upper limit is determined by intracellular optical breakdown, the lower one by the molecular two-photon absorption cross sections of the chromophores and by the detector sensitivity.

In contrast to the CHO results, femtosecond microbeam induced hemolysis showed a dependence on fluence. Because the pulse duration is much shorter than the microsecond thermal relaxation time of the ≈ 8 μ m cell, transient heating in the focal volume and consequent transformations of linear/nonlinear absorbing membrane proteins within the illumination spot may occur resulting in local membrane destruction. No thermal damage is expected in out-of-focus regions, where the steady state thermal distribution is determined by the low mW average power and the temporal pulse separation (12 ns). Therefore, a thermal damage mechanism by highly localized temperature gradients seems to be involved in photoinduced hemolysis. It should be noted, that the pulse duration is too short (no time for molecule collision) to allow the temperature to be defined. A local thermal equilibrium will be reached at some delay after each pulse, but before the next one arrives.

In addition, the enormous peak powers in the W - kW range may induce several orders higher optical forces than in the case of the mW traps. These femtosecond microbeam induced transient μN forces may contribute to membrane damaging effects. Finally, the observed sperm damage reflects UVA-like and CW-NIR-like damage probably induced by oxidative stress due to two-photon excitation of cellular absorbers such as photodynamically active NADH⁸.

In conclusion, the interaction of femtosecond NIR microbeams with vital cells appears to be a complicated process involving a) electric field effects (damage by optical breakdown), b) transient local "temperature" gradients, c) photomechanical stress due to μN force generation, and d) photochemical reactions due to non-resonant nonlinear excitation of endogenous absorbers.

6. REFERENCES

1. A. Ashkin, "Acceleration and Trapping of Particles by Radiation Pressure," *Phys. Rev. Lett.* 24(1970)156-159.
2. A. Ashkin, J.M. Dziedzic, J.E. Bjorkholm, and S. Chu, "Observation of a single-beam gradient force optical trap for dielectric particles," *Opt. Lett.* 11(1986)288-290.
3. W. Denk, J.H. Strickler, and W.W. Webb, "Two-photon laser scanning fluorescence microscopy," *Science* 248(1990)73-76.
4. K. König, T. Krasieva, E. Bauer, U. Fiedler, M.W. Berns, B.J. Tromberg, and K.O. Greulich, "Cell damage by UVA radiation of a mercury microscopy lamp probed by autofluorescence modifications, cloning assay, and comet assay," *J. Biomed. Optics* 1(1996)217-222.
5. K. König, Y. Liu, G.J. Sonek, M.W. Berns, and B.J. Tromberg, "Autofluorescence spectroscopy of optically trapped cells", *Photochem Photobiol.* 62(1995)830-835.
6. K. König, P.T.C. So, W.W. Mantulin, B.J. Tromberg, and E. Gratton, "Two-photon excited lifetime imaging of autofluorescence in cells during UVA and NIR photostress," *J. Microsc.* 183(1996)197-204.
7. R.M. Tyrrell and S.M. Keyse, "The interaction of UVA radiation with cultured cells," *J. Photochem. Photobiol. B* 4(1990)349-361.
8. M.L. Cunningham, J.S. Johnson, S.M. Giovanazzi, and M.J. Peak, "Photosensitized production of superoxide anion by monochromatic (290-405 nm) ultraviolet irradiation of NADH and NADPH coenzymes," *Photochem. Photobiol.* 42(1985)125-128.
9. Y. Liu, D. Cheng, G.J. Sonek, M.W. Berns, C.F. Chapman, and B.J. Tromberg, "Evidence for localized cell heating induced by infrared optical tweezers," *Biophys. J.* 68(1995)2137-2144.
10. K. Svoboda and S.M. Block, "Biological applications of optical forces," *Annu. Rev. Biophys. Biomol. Struct.* 23(1994)247-285.
11. K. König, L.O. Svaasand, Y. Liu, G.J. Sonek, P. Patrizio, Y. Tadir, M.W. Berns, and B.J. Tromberg, "Determination of intrinsic forces of human spermatozoa using an 800 nm optical trap", *Cell.Mol.Biol.* 42(1996)501-509.
12. K. König, H. Liang, M.W. Berns, and B.J. Tromberg, "Cell damage by near-IR microbeams. *Nature* 377(1995)20-21.
13. K. König, H. Liang, M.W. Berns, and B.J. Tromberg, "Cell damage in near-infrared multimode optical traps as a result of multiphoton absorption," *Opt. Lett.* 21(1996)1090-1092.
14. H. Liang, K.T. Vu, P. Krishnan, T.C. Trang, D. Shin, S. Kimel, and M.W. Berns, "Wavelength dependence of cell cloning efficiency after optical trapping", *Biophys. J.* 70(1996)1529-1533.
15. K. König, P.T.C. So, W.W. Mantulin, and E. Gratton, "Cellular response to near-infrared femtosecond laser pulses in two-photon microscopes," *Opt. Lett.* 22(1997) in press.
16. D. von der Linde and H. Schüler, Breakdown thresholds and plasma formation in femtosecond laser-solid interaction," *J.Opt.Soc.Am.B* 13(1996)216-222.
17. J. Rhee, T.S. Sosnowski, T.B. Norris, J.A. Arns, and W.S. Colburn, "Chirped pulse amplification of 85fs pulses at 250 kHz with third-order dispersion compensation by use of holographic transmission gratings," *Opt. Lett.* 19(1994)1550-1552.